



## ORIGINAL RESEARCH

# The cell walls of different *Chara* species are characterized by branched galactans rich in 3-O-methylgalactose and absence of AGPs

Lukas Pfeifer<sup>1</sup>  | Kim-Kristine Mueller<sup>1</sup> | Jon Utermöhlen<sup>1</sup> | Felicitas Erdt<sup>1</sup> |  
Jean Bastian Just Zehge<sup>1</sup> | Hendrik Schubert<sup>2</sup> | Birgit Classen<sup>1</sup> 

<sup>1</sup>Pharmaceutical Institute, Department of Pharmaceutical Biology, Christian-Albrechts-University of Kiel, Kiel, Germany

<sup>2</sup>Aquatic Ecology, Institute of Biosciences, University of Rostock, Rostock, Germany

## Correspondence

Birgit Classen, Pharmaceutical Institute, Department of Pharmaceutical Biology, Christian-Albrechts-University of Kiel, Gutenbergstr. 76, 24118 Kiel, Germany. Email: [bclassen@pharmazie.uni-kiel.de](mailto:bclassen@pharmazie.uni-kiel.de)

## Funding information

Deutsche Forschungsgemeinschaft, Grant/Award Numbers: SCHU 983/23-1, project-number 440046237

Edited by K. Melkonian-Ezekian

## Abstract

Streptophyte algae are the closest relatives to land plants; their latest common ancestor performed the most drastic adaptation in plant evolution around 500 million years ago: the conquest of land. Besides other adaptations, this step required changes in cell wall composition. Current knowledge on the cell walls of streptophyte algae and especially on the presence of arabinogalactan-proteins (AGPs), important signalling molecules in all land plants, is limited. To get deeper insights into the cell walls of streptophyte algae, especially in Charophyceae, we performed sequential cell wall extractions of four *Chara* species. The three species *Chara globularis*, *Chara subspinoso* and *Chara tomentosa* revealed comparable cell wall compositions, with pectins, xylans and xyloglucans, whereas *Chara aspera* stood out with higher amounts of uronic acids in the pectic fractions and lack of reactivity with antibodies binding to xylan- and xyloglucan epitopes. Search for AGPs in the four *Chara* species and in *Nitellopsis obtusa* revealed the presence of galactans with pyranosidic galactose in 1,3-, 1,6- and 1,3,6-linkage, which are typical galactan motifs in land plant AGPs. A unique feature of these branched galactans was high portions of 3-O-methylgalactose. Only *Nitellopsis* contained substantial amounts of arabinose. A bioinformatic search for prolyl-4-hydroxylases, involved in the biosynthesis of AGPs, revealed one possible functional sequence in the genome of *Chara braunii*, but no hydroxyproline could be detected in the four *Chara* species or in *Nitellopsis obtusa*. We conclude that AGPs that is typical for land plants are absent, at least in these members of the Charophyceae.

## 1 | INTRODUCTION

More than 500 million years ago (mya), one of the most significant events for life on Earth occurred: plant terrestrialization (Domozych &

Bagdan, 2022). Land plants (bryophytes, lycophytes, ferns, gymnosperms, and angiosperms) descended from a common algal ancestor that would be classified (if alive today) as a member of the streptophyte algae (Bowman, 2022). Extant streptophyte algae are divided into two grades: the lower-branching KCM-grade (Klebsormidiophyceae, Chlorokybophyceae and Mesostigmatophyceae) and the higher-branching

Lukas Pfeifer and Kim-Kristine Mueller contributed equally to the work.

This is an open access article under the terms of the [Creative Commons Attribution-NonCommercial-NoDerivs](https://creativecommons.org/licenses/by-nc-nd/4.0/) License, which permits use and distribution in any medium, provided the original work is properly cited, the use is non-commercial and no modifications or adaptations are made.

© 2023 The Authors. *Physiologia Plantarum* published by John Wiley & Sons Ltd on behalf of Scandinavian Plant Physiology Society.

ZCC-grade (Zygnematophyceae, Coleochaetophyceae and Charophyceae; de Vries & Archibald, 2018). The genus *Chara* is an important part of the natural aquatic ecosystems, commonly beneficial to lakes and ponds by providing food and cover to wildlife (DiTomaso et al., 2013). Due to the morphological complexity of the Charophyceae, it was first assumed that these streptophyte algae were the closest relatives of extant land plants (Domozych & Bagdan, 2022). However, recent phylogenomic studies have shown that land plants evolved from algal ancestors most closely related to extant Zygnematophyceae (Domozych & Bagdan, 2022; Leebens-Mack et al., 2019; Wickett et al., 2014). This group of streptophyte algae is further classified in a recently proposed five-order system of Desmidiiales, Spirogyrales, Zygnematales, Serritaeiales and Spiroglaoales (Hess et al., 2022).

To cope with life on land, the terrestrial algal species had to adapt to enormous changes in the environment, such as UV radiation and drought. This also meant that the cell wall needed to adapt by changing its composition (Harholt et al., 2016). The plant cell wall is generally a highly dynamic system consisting mainly of polysaccharides and cell wall proteins. It has many essential functions, such as mechanical stability and protection against abiotic and biotic stressors (Silva et al., 2020). The main polysaccharides of spermatophyte cell walls include cellulose, pectins, hemicelluloses and lignin. Hemicelluloses are cross-linked in a highly branched network of cellulose microfibrils, which are embedded in a matrix of pectins (Sørensen et al., 2011). Important cell wall proteins are hydroxyproline-rich glycoproteins (HRGPs). These comprise arabinogalactan-proteins (AGPs), proline-rich proteins (PRPs) and extensins (EXT; Johnson et al., 2018), differing mainly in their carbohydrate moiety. While the glycan part is about 90% in AGPs, it is about 50% in EXT. In PRPs, the protein part is only marginally glycosylated (Johnson et al., 2018).

The AG moiety of AGPs consists of arabinogalactans type II (AG II) with a (1 → 3)-β-D-galactan core structure carrying (1 → 6)-β-D-galactan side chains at position O-6. These side chains are decorated with α-L-Araf and other monosaccharides, like L-Rha, L-Fuc or D-GlcAp (Kitazawa et al., 2013). AGs in AGPs are covalently linked to the protein moiety via hydroxyproline (Hyp). The hydroxylation of Pro to Hyp is post-translationally catalyzed by prolyl-4-hydroxylase (P4H; Seifert et al., 2021).

Additionally, a glycosylphosphatidylinositol (GPI)-anchor can be attached at the C-terminal side, which connects the AGP to the plasma membrane (Silva et al., 2020). There are descriptions of AGPs as periplasmic calcium capacitors proposing AGPs as being important partners in calcium signalling (Lampert, 2023; Lampert & Várnai, 2013). Even if it is not yet fully explained how the signal transmission of AGPs takes place, the periplasmic localization facilitates this process. AGPs of seed plants show many diverse functions, which include cell growth, pattern formation, salt- and drought-tolerance, cell-cell communication or adhesiveness (for review, see Ma et al., 2018; Mareri et al., 2018; Leszczuk et al., 2023; Seifert & Roberts, 2007). Because of these functions, AGPs are ideal candidates for molecules that are essential for life on land and may, therefore, have evolved in the last common ancestor of all streptophytes. Ferns and bryophyte have the same general AGP structure as known from

seed plants, but shows unique variations in the carbohydrate part, e.g. the presence of 3-O-methylrhamnose as terminal monosaccharide (Bartels et al., 2017; Bartels & Classen, 2017; Fu et al., 2007; Mueller et al., 2023). Whether AGPs (i.e. typical protein backbones with typical glycosylation) are present in the different algae lineages is still questionable. Based on bioinformatics screenings of transcriptomes, protein backbones of AGPs have been identified in brown, red and green algae (Johnson et al., 2017). Furthermore, AGP glycan epitopes have been detected by monoclonal antibodies in brown (Hervé et al., 2016; Raimundo et al., 2016) and green algae, including some streptophyte algae (Domozych et al., 2009; Eder et al., 2008; Estevez et al., 2008; Estevez et al., 2009; Palacio-López et al., 2019; Permann, Herburger, Felhofer, et al., 2021; Permann, Herburger, Niedermeier, et al., 2021; Přerovská et al., 2021; Ruiz-May et al., 2018; Sørensen et al., 2011). Nevertheless, it remains open whether epitopes are linked to the characteristic protein backbones.

To the best of our knowledge, no AGPs similar to the ones in land plants have been isolated from streptophyte algae to date. Closely related rhamnogalactan-proteins (RGPs) are present in the cell walls of *Spirogyra pratensis*, a member of the Zygnematophyceae (Pfeifer et al., 2022). These RGPs reveal typical AGP features like a Hyp-rich protein moiety covalently bound to 1,3-, 1,6- and 1,3,6-linked galactans and the ability to precipitate with Yariv's reagent. Interestingly, there is a nearly complete replacement of arabinose by rhamnose at the periphery of these RGPs, leading to a less hydrophilic surface, which may be connected with different functions in the freshwater habitat (Pfeifer et al., 2022). To continue the search for evolutionary roots of AGPs or AGP-like molecules in streptophytes, we searched for these glycoproteins in four *Chara* species (Charophyceae). As hydroxylation of proline is the basis for O-glycosidic linkage between protein- and carbohydrate moiety in AGPs, we also performed a bioinformatic search for P4Hs. The work is complemented by sequential extraction of *Chara* cell walls to get insights into the general cell wall polysaccharide composition of this genus. The results broaden our general understanding of cell walls of the higher branching streptophyte algae and further enlighten the process of cell wall evolution from algae to land plants.

## 2 | MATERIALS AND METHODS

### 2.1 | Plant material and sampling

The streptophyte algae *Chara globularis* THUILL., *Chara subspinoso* RUPR. and *Chara tomentosa* L. were collected in June 2018 in the lake “Lüt-zlower See” in Uckermark (53°14'45.9" N, 14°01'54.2" E; Germany). *Chara aspera* WILLD. was collected in July 2021 in the lake in Lalendorf (53°40'33.2" N, 12°26'05.9" E; Germany). All samples were cleaned with water and freeze-dried (Christ Alpha 1–4 LSC, Martin Christ Gefriertrocknungsanlagen GmbH). Preliminary experiments were carried out with *C. subspinoso* from the Lunzer See and *C. tomentosa* and *C. globularis* from the Neusiedler See. The Austrian samples were collected and identified by Prof. Dr Michael Schagerl and Barbara

Mährert from the Department for Limnology and Oceanography of the University of Wien. Previously studied samples of *Echinacea purpurea* (Classen et al., 2004) and *Nitellopsis obtusa* (Pfeifer et al., 2022) were additionally used for comparison and were treated similarly to the *Chara* samples for experiments missing in the original publications.

## 2.2 | Isolation of cell wall fractions

The freeze-dried and ground plant material was pre-extracted two times (2 h and 21 h) with 70% acetone solution (v/v) in a 1:10 (w/v) ratio. After drying, the plant residue was extracted with double-distilled water (ddH<sub>2</sub>O) for 21 h under constant stirring (SM 2484, Edmund Bühler GmbH) at 4°C in a 1:10 (w/v) ratio. The aqueous extract was separated with a tincture press (HAFICO HP 2 H, Fischer Tinkturenpressen GmbH) and the insoluble plant pellet was freeze-dried for further extractions (see below).

After heating the aqueous extract in a water bath (GFL 1002, LAUDA-GFL Gesellschaft für Labortechnik mbH) at 90–95°C for 10 min, the denatured proteins were removed by centrifugation (4122 g, 20 min, 4°C, Heraeus Multifuge X3R, Thermo Scientific Inc.). To precipitate polysaccharides and AGPs, the aqueous extract was first evaporated in a rotary evaporator (40°C, 0.010 mbar; Laborota 4000, Heidolph Instruments GmbH & CO.) to approximately one-tenth of its volume and subsequently added to cooled ethanol resulting in a final concentration of 80% (v/v). After incubation overnight at 4°C, the precipitate was isolated by centrifugation (4°C, 19,000 g, 20 min) and finally freeze-dried (AE).

To remove starch, approximately 100 mg of AE were treated with  $\alpha$ -amylase + amyloglucosidase ( $\alpha$ -amylase from *Aspergillus oryzae*, EC number 3.2.1.1., 15 U mg<sup>-1</sup> polysaccharide; amyloglucosidase from *Aspergillus niger*, EC number 3.2.1.3., 7 U mg<sup>-1</sup> polysaccharide; both from Sigma-Aldrich Chemie GmbH; in 50 mmol L<sup>-1</sup> acetate buffer at pH 5.2, 50°C for 20 h). Subsequently, the samples were treated with pectinase (Sigma-Aldrich Chemie GmbH, from *A. niger*, EC number 3.2.1.15., 1  $\mu$ L mg<sup>-1</sup>, for 5 h, in 50 mmol L<sup>-1</sup> acetate buffer at pH 5.2, 37.5°C) to cleave homogalacturonan parts. The enzymes were removed by heating in a boiling water bath for 10 min with the following centrifugation at 19,000 g for 20 min. Afterwards, the samples were dialyzed against demineralized water (4°C; 4 d; MWCO 12–14 kDa, Visking®, Mediatech International Ltd) and freeze-dried (AE<sub>AP</sub>).

According to a modified method of O'Rourke et al. (2015) and Raimundo et al. (2016), the insoluble plant pellet after water extraction (see above) was used for the isolation of four additional polysaccharide fractions.

The pellet was subsequently extracted with ammonium oxalate ((NH<sub>4</sub>)<sub>2</sub>C<sub>2</sub>O<sub>4</sub>, 0.2 mol L<sup>-1</sup>), hydrochloric acid (HCl, 0.01 mol L<sup>-1</sup>), sodium carbonate (Na<sub>2</sub>CO<sub>3</sub>, 3% (w/v)) and potassium hydroxide (KOH, 2 mol L<sup>-1</sup>), each in a ratio of 1:100 (w/v) at 70°C under constant stirring for 21 h (RET basic, ETS D5, IKA Labortechnik, Staufen, Germany). The pellet and the supernatant were separated after each

extraction by centrifugation (4°C, 19,000 g, 20 min, Heraeus Multifuge X3, Thermo Fisher Scientific Corp.).

To precipitate the Na<sub>2</sub>CO<sub>3</sub> fraction, the supernatant was added to acetone in a 1:4 (V/V) ratio. After incubation overnight at 4°C, the precipitated material was re-dissolved in ddH<sub>2</sub>O in a 1:100 (w/v) ratio. The KOH extract was neutralized (761 Calimatic, Knick Elektronische Messgeräte GmbH & Co. KG). All fractions were dialyzed against demineralized water (4°C, 4 d, MWCO 12–14 kDa, Visking®) and freeze-dried. The whole workflow is schematically represented in Figure S1.

## 2.3 | Analysis of monosaccharides

The neutral monosaccharide composition was determined by the method of Blakeney et al. (1983) with slight modifications (see Mueller et al., 2023). Gas chromatography (GC) with flame ionization detection (FID) and mass spectrometry (MS) detection were used to identify and quantify the neutral monosaccharides: GC + FID: 7890B; Agilent Technologies Inc.; MS: 5977B MSD; Agilent Technologies, USA; column: Optima-225; Macherey-Nagel GmbH & Co. KG; 25 m, 250  $\mu$ m, 0.25  $\mu$ m; helium flow rate: 1 mL min<sup>-1</sup>; split ratio 30:1. A temperature gradient was performed to achieve peak separation (initial temperature 200°C, subsequent holding time of 3 min; final temperature 243°C with a gradient of 2°C min<sup>-1</sup>). The methylated monosaccharide 3-O-MeRha was identified by retention time and mass spectrum (see Happ & Classen, 2019), 3-O-MeFuc was determined using the mass spectrum and the deviating retention time to 3-O-MeRha. 3-O-MeGal was also quantified by mass spectrum, but additionally, the validated method of Pfeifer and Classen (2020) was used to distinguish 3-O-MeGal from 4-O-MeGal.

The uronic acid (UA) compounds were determined photometrically at 525 nm (UVmini-1240, Shimadzu AG) according to the method of Blumenkrantz and Asboe-Hansen (1973), for modifications, see Mueller et al. (2023).

## 2.4 | Carboxy-reduction of uronic acids

The method of Taylor and Conrad (1972), with slight modifications, was used to perform a carboxy-reduction of the uronic acids of the AE<sub>AP</sub> fractions. Firstly, 20–30 mg AE<sub>AP</sub> were dissolved in 20 mL ddH<sub>2</sub>O and 216 mg of *N*-cyclohexyl-*N'*-[2-(*N*-methylmorpholino)ethyl]-carbodiimide-4-toluenesulfonate was added slowly under constant stirring. An autotitrator (Metrohm 719 S-Titrino, Deutsche METHROM GmbH & Co. KG) adjusted the pH to 4.75 with 0.01 M HCl for 2 h. One to two drops of 1-octanol were added to avoid strong foaming. Sodium borodeuteride solutions (in ddH<sub>2</sub>O) were added in increasing concentrations (4.0 mL of 1 mol L<sup>-1</sup>; 5 mL of 2 mol L<sup>-1</sup>; 5 mL of 4 mol L<sup>-1</sup>) to carboxy-reduce the uronic acids. The autotitrator adjusted the pH to 7.00 with 2 M HCl for another 2 h. After pH setting to 6.5 with glacial acetic acid, the solutions were dialyzed for three days at 4°C against demineralized water (MWCO 12–14 kDa, Visking®) and freeze-dried.

## 2.5 | Structural characterization of water-soluble polysaccharides

Following the method of Harris et al. (1984; see Mueller et al., 2023 for modifications), structural characterization of the polysaccharides was performed. Potassium methylsulfinyl carbanion (KCA) and iodomethane- $d_3$  (IM- $d_3$ ) were added to the samples in a defined scheme to methylate the samples (1) 100  $\mu$ L KCA for 10 min; (2) 80  $\mu$ L IM- $d_3$  for 5 min; (3) 200  $\mu$ L KCA for 30 min; (4) 150  $\mu$ L IM- $d_3$  for 60 min. After following hydrolysis, reduction, and acetylation, the samples were modified to permethylated alditol acetates (PMAA). These were identified by GC-MS (instrumentation see above: Section 2.3; column: Optima-1701, 25 m, 250  $\mu$ m, 0.25  $\mu$ m; helium flow rate: 1 mL  $\text{min}^{-1}$ ; initial temperature: 170°C; hold time 2 min; rate 1°C  $\text{min}^{-1}$  until 210°C was achieved; rate: 30°C  $\text{min}^{-1}$  until 250°C was achieved; final hold time 10 min) by their retention times and comparison to a PMAA library established in the working group.

## 2.6 | Determination of hydroxyproline content

For Hyp quantification, the methodology of Stegemann and Stalder (1967) was used in a modified version (see Mueller et al., 2023). The Hyp content was measured colourimetrically at 558 nm and quantified via a linear regression analysis with a Hyp standard.

## 2.7 | Indirect enzyme-linked immunosorbent assay (ELISA)

First, 96-well plates (Nunc-Immuno<sup>®</sup> Plates, Thermo Scientific) were coated with 100  $\mu$ L per well of the sample in triplicate (concentrations in ddH<sub>2</sub>O: 12.5  $\mu$ g  $\text{mL}^{-1}$  for  $[\text{NH}_4]_2\text{C}_2\text{O}_4$  and KOH; 12.5  $\mu$ g  $\text{mL}^{-1}$ , 25  $\mu$ g  $\text{mL}^{-1}$  50  $\mu$ g  $\text{mL}^{-1}$  for AE). Afterwards, these were incubated at 37.5°C for 3 days. A negative control of ddH<sub>2</sub>O was used and treated likewise. The plates were washed three times with 100  $\mu$ L phosphate buffered saline (PBS)-T (pH 7.4, 0.05% Tween<sup>®</sup> 20) per well and blocked with 200  $\mu$ L of BSA (bovine serum albumin, 1%, w/v) in PBS per well. After incubation at 37.5°C for 1 h, the plates were washed again three times. Following the addition of 100  $\mu$ L of primary antibody solution (INRA-RU2, 1:200 dilution; JIM13, 1:40 dilution; KM1, LM2, LM6, LM10, LM15, LM19, 1:20 dilution) per well in PBS 7.4 dilution, the plates were incubated again (1 h at 37.5°C). After washing three times again, the procedure was repeated for the secondary antibody (anti-mouse-IgG for INRA-RU2 and KM1; anti-rat-IgG for all other antibodies; both produced in goat and conjugated with alkaline phosphatase, Sigma-Aldrich Chemie GmbH) in a ratio of 1:500 (v/v) in PBS 7.4. Subsequently, the substrate solution of *p*-nitro-phenylphosphate was added (100  $\mu$ L well<sup>-1</sup>). The plates were incubated at room temperature in the dark, and the absorbance was determined at 405 nm with a plate reader (Infinite F50 Plus, Tecan Group Ltd.) after 40 min. For visualization purposes, the absorbance of the control was set to 0 and the highest signal in the dataset was set to 1.0. Epitopes of the antibodies and key references are listed in Table S1.

## 2.8 | Gel diffusion assay

For the gel diffusion assay, an agarose gel (Tris-HCl, 10 mmol  $\text{L}^{-1}$ ; CaCl<sub>2</sub>, 1 mmol  $\text{L}^{-1}$ ; NaCl, 0.9% w/v; agarose, 1% w/v) was used, in which several cavities were stamped in. The cavities in the first and third rows were filled with dilutions (100 mg  $\text{mL}^{-1}$ ) of the samples. In the second line, the cavities left and right were filled with the positive control, AGP from *Echinacea purpurea* (10 mg  $\text{mL}^{-1}$ ), and the middle cavities with the  $\beta$ GlcY solution (1 mg  $\text{mL}^{-1}$ ). The assay was incubated for 22 h in the dark. If AGPs are present in the samples, a red precipitation line appears, as in the positive control.

## 2.9 | Bioinformatic search for prolyl-4-hydroxylase (P4H)

Candidate sequences for P4Hs were obtained from the translated proteome of *Chara braunii* (Nishiyama et al., 2018; [https://plants.ensembl.org/Chara\\_braunii/Info/Index](https://plants.ensembl.org/Chara_braunii/Info/Index), v1.0) under the use of the R package rBLAST (Hahsler & Nagar, 2019) with the *Arabidopsis thaliana* P4Hs as query sequences. An E-value of  $1e^{-7}$  was used and the resulting candidates were aligned with functionally described P4H sequences (Hieta & Myllyharju, 2002; Keskiäho et al., 2007; Vlad et al., 2010; Velasquez et al., 2015; Yuasa et al., 2005) by the use of MAFFT in L-INS-i mode (Kato & Standley, 2013). The occurrence of relevant amino acids was evaluated in comparison to *Chlamydomonas reinhardtii* P4H1. Afterwards, some sequences were modelled with the SWISS-MODEL web server (Waterhouse et al., 2018) with default settings on the JIG2/A crystal structure of *C. reinhardtii* P4H (Koski et al., 2007).

## 3 | RESULTS

### 3.1 | Sequential extraction of polysaccharide fractions from *Chara* spp. cell walls

We examined four *Chara* species to investigate their cell wall compositions. Sequential extraction of the plant material with water (AE), ammonium-oxalate ( $[\text{NH}_4]_2\text{C}_2\text{O}_4$ ) and hydrochloric acid (HCl), as well as sodium carbonate ( $\text{Na}_2\text{CO}_3$ ) and potassium hydroxide (KOH), resulted in a water-soluble, two pectic and two hemicellulosic fractions. The yields of the different fractions varied between 0.2% and 21.2% of the dry plant material (Table S2). The high yield of the  $[\text{NH}_4]_2\text{C}_2\text{O}_4$  fraction of *Chara aspera* (21.2%) was striking and indicated huge amounts of pectins in this species.

### 3.2 | Pectic fractions of *Chara* spp. cell walls

The monosaccharide compositions of the pectic fractions are shown in Tables 1, S3A and S3B and Figure 1. As expected, the two pectic

fractions showed the highest amounts of uronic acids. In the  $(\text{NH}_4)_2\text{C}_2\text{O}_4$  fractions, the content reached 33% to 60% of the dry fraction material and decreased in the HCl fractions of all investigated *Chara* spp. (Table 1).

**TABLE 1** Colorimetric determination of the content of uronic acids in the different cell wall fractions from different *Chara* species in % ( $\text{w w}^{-1}$ ).

	<i>C. aspera</i>	<i>C. globularis</i>	<i>C. subspinosa</i>	<i>C. tomentosa</i>
AE	5.8	3.4	3.6	4.2
$(\text{NH}_4)_2\text{C}_2\text{O}_4$	60.6 ± 1.7	33.1 ± 1.2	50.9 ± 2.5	42.8 ± 4.1
HCl	39.4 ± 8.5	7.1	8.2	11.3
$\text{Na}_2\text{CO}_3$	7.6	4.8	6.3	10.0
KOH	6.0	7.1	5.3	6.1

In contrast to the other *Chara* species, the uronic acid content in *C. aspera* was the highest, with over 60% in the  $(\text{NH}_4)_2\text{C}_2\text{O}_4$  and almost 40% in the HCl fraction. The dominant neutral monosaccharide in both fractions was Glc, with 25 to 66% (Tables S3A and S3B). In the HCl fractions, the content was approximately doubled in *C. globularis* and *C. subspinosa* compared to the corresponding  $(\text{NH}_4)_2\text{C}_2\text{O}_4$  fractions. It cannot be excluded that at least part of the Glc derived from coextracted starch. Other monosaccharides, like Rha, Gal and Ara present in rhamnogalacturonan-I (RG-I) or Xyl part of xylogalacturonan (XG), were also detected in these fractions. High amounts of Xyl, especially in *C. tomentosa* and substantial amounts of Fuc and Man in all fractions indicate that further polysaccharides besides pectins are present in these fractions. A very unusual feature, present mainly in the  $(\text{NH}_4)_2\text{C}_2\text{O}_4$  fractions, is 3-O-MeGal, especially prominent in *C. aspera*.

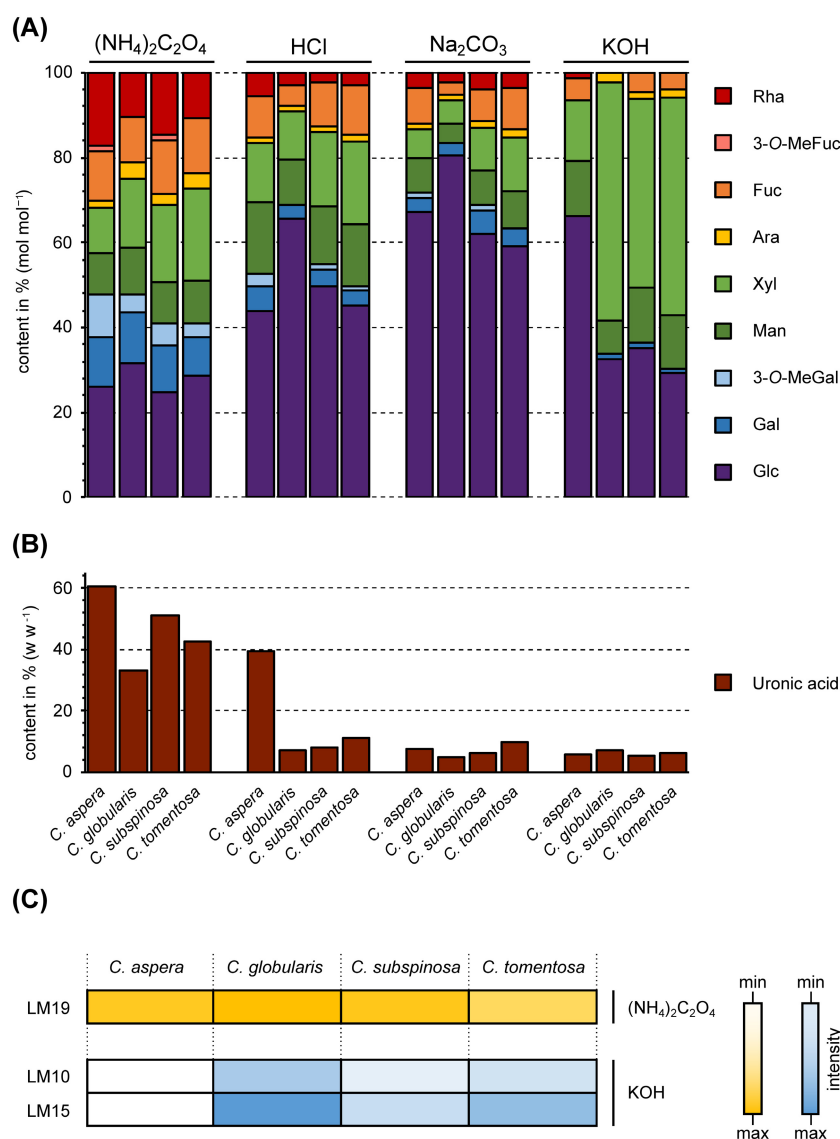


**FIGURE 1** Monosaccharide composition of different cell wall fractions ( $(\text{NH}_4)_2\text{C}_2\text{O}_4$ , HCl,  $\text{Na}_2\text{CO}_3$ , KOH) from the streptophyte algae *C. aspera*, *C. globularis*, *C. subspinosa* and *C. tomentosa*. (A) Relative neutral monosaccharide composition determined by gas chromatography (GC; % mol mol<sup>-1</sup>). (B) Absolute content of uronic acids determined by colorimetric assay ( $\text{w w}^{-1}$  of dry fraction weight). (C) Reactivity of *Chara* spp. fractions with antibodies via ELISA after 40 min in the concentration 12.5  $\mu\text{g mL}^{-1}$  ( $(\text{NH}_4)_2\text{C}_2\text{O}_4$ : LM19; KOH: LM10, LM15).

To confirm the presence of pectins, the antibody LM19 raised against unesterified HG epitopes (Verhertbruggen, Marcus, Haeger, Ordaz-Ortiz, & Knox, 2009) was tested for binding affinity to the  $(\text{NH}_4)_2\text{C}_2\text{O}_4$  fractions (Figure 1), which revealed comparable amounts of unesterified HG in all *Chara* species. The antibody INRA-RU2, which recognizes the RG-I backbone (Ralet et al., 2010) showed no affinity to the  $(\text{NH}_4)_2\text{C}_2\text{O}_4$  and the AE\_AP fractions of all *Chara* species (Figure S2).

### 3.3 | Hemicellulosic fractions of *Chara* spp. cell walls

Glc was dominating the sodium carbonate fractions (Table S3C) with 59% to 80%. All other monosaccharides were present in amounts less than 10% (except 12.7% Xyl in *C. tomentosa*), indicating the occurrence of mainly glucans in these fractions.

The KOH fractions (Table S3d) was dominated by Xyl and Glc, accompanied by Man. In all species, Xyl and Glc accounted for a minimal of 80% of the neutral monosaccharides, while the ratio of Xyl: Glc varied. Again, *C. aspera* was stood out, with a very low Xyl content in this fraction. The occurrence of xylan and xyloglucan was supported by ELISA with the antibodies LM10 and LM15. These antibodies detect the epitopes of the non-reducing end of  $(1 \rightarrow 4)\text{-}\beta\text{-D-xylan}$  (LM10; McCartney et al., 2005; Ruprecht et al., 2017), as well as the XXXG-motif of xyloglucan (LM15; Marcus et al., 2008; Pedersen et al., 2012). The highest absorption with both antibodies was detectable in *C. globularis*, followed by *C. tomentosa* and *C. subspinosa*. *C. aspera* revealed no binding to one of these antibodies.

### 3.4 | Search for AGPs in *Chara* spp. cell walls

Water-soluble polysaccharides were precipitated with ethanol 80% (AE) and consisted mainly of Gal (including 3-O-MeGal) and Glc (Table S4A). The amounts of uronic acids in AE were quantified photometrically and varied between 3.4% and 5.8% (Table 1). In preliminary experiments, precipitation of AE with Yariv's reagent yielded no AGP-like monosaccharide composition. The precipitate was had a similar composition as AE, with only a slight increase in Gal content (data not shown). Therefore, we used enzymatic treatments to purify putative AGPs, which might be present in AE in very minor amounts. As starch and some pectins might have been coextracted with these AGP-like galactan structures, we treated AE fractions with  $\alpha$ -amylase and pectinase, precipitated the remaining polysaccharides with ethanol 80% and dialyzed the precipitates to remove residual mono- or oligosaccharides (Table S4B). These treatments led to a decrease in Glc and an increase in Gal content in all species (compare Tables S4A and S4B). Comparable to the  $(\text{NH}_4)_2\text{C}_2\text{O}_4$  fraction, the highest amount of 3-O-MeGal, with 19.3%, was found in *C. aspera*. The monosaccharides Rha, Fuc, Xyl and Man were distributed in quite similar quantities, between 7.5% and 16.5%, in all investigated *Chara* species, whereas the amounts of Ara were relatively low (2.2% and 4.0%). Compared to the different *Chara*

species, *N. obtusa* was richer in Rha and Ara. To detect uronic acids, samples were carboxy-reduced by the use of sodium borodeuteride. There were only slight increases in Gal and Glc (compare Table S4B and Table 2). The mass spectra showed deuterated fragments deriving from GlcA and, to a lesser extent, from GalA.

#### 3.4.1 | Gel diffusion assay

A typical feature of AGPs is the precipitation with Yariv phenyl glycosides, like  $\beta\text{-D-glucosyl Yariv-reagent}$  ( $\beta\text{GlcY}$ ). A gel diffusion assay provides a first hint of whether AGPs are present in the sample. If AGPs are included, a red precipitation line will appear between the sample and the  $\beta\text{GlcY}$  (Clarke et al., 1978). The water-soluble fractions (AE) of all *Chara* species showed no Yariv precipitation, but after enzymatic treatment, weak precipitation lines were observed for all *Chara* species but not for *Nitellopsis obtusa*, another member of the Charophyceae (Figure S3).

#### 3.4.2 | Structure elucidation

The purified aqueous extracts (AE\_AP, see Sections 2 and 2.2) of all *Chara* species and of *N. obtusa* were subjected to linkage-type analysis (Table 3) to gain insight into the polysaccharides present. Galp as the main monosaccharide was present as terminal residue (1.3%–4.4%), in 1,3-linkage (6.7%–13.6%), 1,6-linkage (5.1%–41.6%) and 1,3,6-linkage (4.5%–13.2%). Interestingly, these are the typical Gal linkage types present in land plant AGPs. To identify the linkage types of 3-O-MeGal, permethylation was carried out by using IM-d<sub>3</sub>. Mass spectra (GC-MS after acetylation) clearly revealed that some of the terminal and also 1,6-linked Galp residues are present as 3-O-MeGal in the non-reduced samples. Typical AGP linkage types of Araf (terminal and 1,5-linked Ara) in higher amounts were present only in *N. obtusa* AE\_AP. All samples and especially that of *N. obtusa* were further characterized by high amounts of 1,4-linked Rhap, accompanied by small amounts of other linkage types of this monosaccharide. Further components of the samples were Glc/GlcA, Fuc and Xyl as terminal residues and further linkage types of desoxyhexoses (Rha and/or Fuc) and hexoses (Man and Glc). The mass spectrum of terminal Glc in the uronic acid reduced sample clearly showed additional  $m/z +2$  in the primary fragments containing the original carboxyl group at C6. These deuterated fragments revealed the presence of GlcA in the native sample. The peak of 1,4-Hexp also contained small amounts of deuterated fragments, thus revealing the presence of 1,4-GalA or 1,4-GlcA (same retention time) in the native sample.

#### 3.4.3 | ELISA with antibodies directed against AG glycan epitopes

Four AE fractions were tested for binding affinities to the antibodies JIM13, KM1, LM2 and LM6 (Figure 2) with the aim to detect AG-glycan structures.

**TABLE 2** Neutral monosaccharide composition of dialyzed water-soluble polysaccharides, pre-treated with amylase and pectinase after reduction of uronic acids (AE\_AP\_UR), from different *Chara* species and *Nitellopsis obtusa* in % (mol mol<sup>-1</sup>; tr: trace value < 1%; n = 3).

Neutral monosaccharide	<i>C. aspera</i> AE_AP_UR	<i>C. globularis</i> AE_AP_UR	<i>C. subspinoso</i> AE_AP_UR	<i>C. tomentosa</i> AE_AP_UR	<i>N. obtusa</i> AE_purified_AP_UR
Rha	12.6 ± 0.1	10.7 ± 0.2	13.7 ± 0.2	10.0 ± 0.2	18.6 ± 0.3
3-O-MeFuc	-	-	1.9 ± 0.1	-	-
Fuc	8.7 ± 0.0	14.1 ± 0.1	8.7 ± 0.2	11.6 ± 0.1	6.4 ± 0.0
Ara	2.1 ± 0.1	3.7 ± 0.1	2.3 ± 0.1	2.1 ± 0.1	14.4 ± 0.1
Xyl	6.7 ± 0.4	8.6 ± 0.1	9.7 ± 0.0	12.8 ± 0.8	5.1 ± 0.0
Man	9.0 ± 0.1	9.9 ± 0.1	10.7 ± 0.2	12.8 ± 0.2	8.0 ± 0.2
3-O-MeGal	21.3 ± 0.3	8.1 ± 0.2	10.1 ± 0.1	4.7 ± 0.2	2.5 ± 0.0
Gal	18.3 ± 0.2	22.4 ± 0.2	20.2 ± 0.4	16.7 ± 0.1	26.8 ± 0.0
Glc	21.3 ± 0.7	22.5 ± 0.2	22.7 ± 0.2	29.3 ± 0.4	18.2 ± 0.1

**TABLE 3** Linkage type analysis of AE\_AP from *Chara* spp. and *N. obtusa* in % (w w<sup>-1</sup>, n = 1).

Monosaccharide	Linkage type	<i>C. aspera</i> AE_AP	<i>C. globularis</i> AE_AP	<i>C. subspinoso</i> AE_AP	<i>C. tomentosa</i> AE_AP	<i>N. obtusa</i> AE_AP
Galp	1,3,6-	7.0	5.7	6.0	4.5	13.2
	1,3-	6.7	9.0	9.7	9.0	13.6
Galp/3-O-MeGalp	1,6-	41.6	13.9	11.1	5.1	10.0
	1-	4.2	4.4	2.8	2.7	1.3
GlcP	1,3-	1.0	4.1	3.7	5.9	2.1
	1-	5.1	7.7	8.4	11.8	2.6
Hexp	1,2,4,6-	1.8	2.8	5.0	3.6	-
	1,4,6-	-	2.4	2.2	1.7	1.1
	1,3,4-	-	3.2	2.4	4.9	1.0
	1,2,6-	-	3.4	5.0	7.5	4.3
	1,4-	3.3	7.3	6.2	6.4	4.4
Rhap	1,2-	3.1	5.2	4.7	5.5	2.1
	1,2,4-	-	1.0	tr	tr	1.0
	1,4-	15.5	9.1	12.4	10.7	19.7
	1,2-	1.4	1.8	1.4	1.5	0.0
Fucp	1-	1.9	2.3	2.6	2.2	4.0
	1-	4.4	5.8	9.3	7.2	3.4
Desoxyhexp	1,3,4-	-	3.1	tr	tr	-
	1,3-	-	1.7	1.3	1.8	1.3
Araf	1,5-	-	-	-	-	5.6
	1-	1.2	1.6	1.3	1.2	6.8
Xylp	1-	1.8	4.5	4.5	7.1	2.5

For JIM13 (Figure 2A), the exact epitope is still under debate. It is accepted as a typical AGP antibody, and Rha and uronic acids might be part of the epitope (Pfeifer et al., 2022). The trisaccharide β-D-GlcAp-(1 → 3)-α-D-GalAp-(1 → 2)-α-L-Rha has been shown to bind to JIM13 (Yates et al., 1996). The affinity of JIM13 to AE of all *Chara* species was strong, concentration-dependent and comparable between the species with slightly weaker binding of the AE of *C. tomentosa*.

The antibody KM1 (Figure 2B) detects (1 → 6)-β-D-Galp units in AGs type II (Classen et al., 2004; Ruprecht et al., 2017). LM2 (Smallwood et al., 1996, Figure 2C) recognizes (1 → 6)-β-D-Galp units with terminal β-D-GlcAp present in AGPs (Ruprecht et al., 2017) and showed moderate binding properties to AE of *C. globularis* and *C. subspinoso*, but very strong reactivity with AE of *C. aspera*. This species contains the highest amounts of 1,6-linked Gal (Table 3). In contrast, the AE of *C. tomentosa* demonstrated a weaker binding. LM6

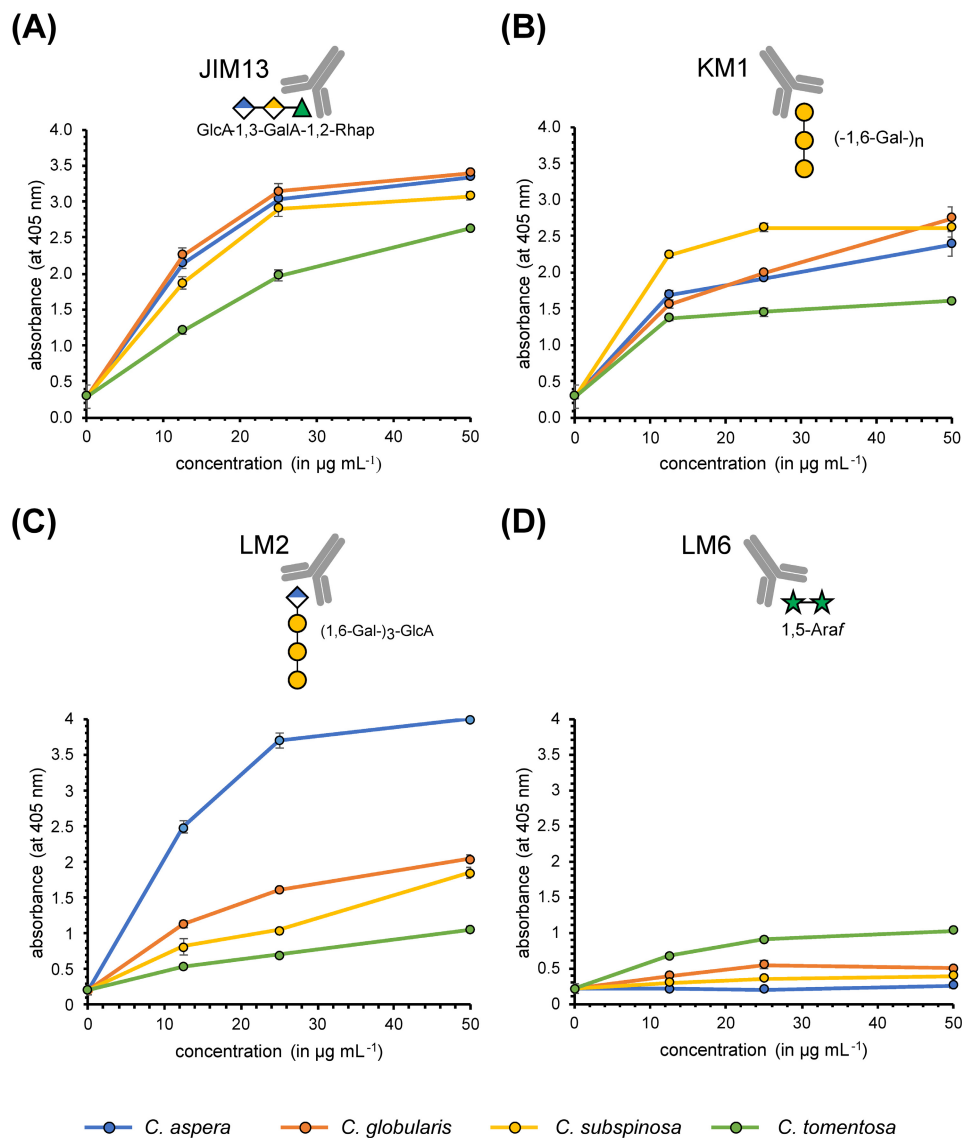


**FIGURE 2** Reactivity of monoclonal antibodies with polysaccharide structures in AEs of different *Chara* species determined via ELISA. Antibodies are directed against typical AGP glycan structures, which are briefly symbolized above each diagram. (A) JIM13; (B) KM1; (C) LM2; (D) LM6. For epitopes of the antibodies, see Table S1.

(Figure 2D) identifies (1 → 5)- $\alpha$ -L-Araf oligomers in arabinans or AGPs (Verhertbruggen, Marcus, Haeger, Verhoef, et al., 2009). The AE of *C. tomentosa* showed weak binding to LM6, whereas the other *Chara* species showed no reactivity. Low or no affinity to this antibody is in accordance with low Ara content in the AE of these species (Table 3).

### 3.4.4 | Quantification of hydroxyproline

Most arabinogalactans are covalently linked to a protein backbone via the amino acid Hyp. According to Stegemann and Stalder (1967), the Hyp contents of all *Chara* AE samples were quantified photometrically. The results were striking, as Hyp was not detectable in any of the samples. Samples (AE) of *C. globularis*, *C. subspinoso*, *C. tomentosa*

(collected in Austria), as well as from *N. obtusa*, showed no detectable Hyp. Therefore, the question of whether P4Hs are present in the genome of *C. braunii* arose.

### 3.4.5 | Bioinformatic search for prolyl-4-hydroxylase

A BLAST search of the available genome data of *C. braunii* revealed the presence of seven putative P4H homologs. In a detailed analysis of the aligned sequences, the absence or presence of relevant amino acids in the oxoglutarate-binding site as well as the iron-binding region (according to Hieta & Myllyharju, 2002; Keskiho et al., 2007; Koski et al., 2007; Koski et al., 2009) was investigated (Table S5A and S5B; Data S1). Only in two cases, all important residues were found





diverging structures in the putative substrate binding channel of *C. braunii* P4H in comparison to AtP4H1 and CrP4H (see red and green boxes in Figure 3H). Some of these structural differences (Pro instead of Asp<sup>149</sup>; Tyr instead of Asn<sup>152</sup>) are also visible in some of the P4H sequences used for comparison (AtP4H13 and NtP4H1.2). Both substrate channel regions, the  $\beta$ 3- $\beta$ 4 loop as well as the  $\beta$ II- $\beta$ III loop, contain flexible parts which show a low degree of alignment (Figure 3B-H) flanked with phylogenetically highly conserved amino acids.

## 4 | DISCUSSION

### 4.1 | Polysaccharides of *Chara* cell walls

Although taxonomically differences in cell wall composition become more and more defined, knowledge on streptophyte algal cell walls is still limited. There is some evidence for the occurrence of nearly all seed plant polysaccharides in streptophyte algae (Domozych & Bagdan, 2022), but recent studies are often based on immunocytochemistry. This approach has limitations as epitopes of antibodies are not always clearly defined. Thus, isolation and analytical characterization of cell wall polysaccharide fractions of streptophyte algae as closest living relatives to land plants help to understand cell wall evolution during plant terrestrialization.

### 4.2 | Pectin composition in Charales hints towards presence of (substituted) HGs, but absence of RG-I

For the isolation of pectic fractions, we used standard procedures with chelators and hot acid (Scheller & Ulvskov, 2010). The high amount of the  $(\text{NH}_4)_2\text{C}_2\text{O}_4$  fraction in *C. aspera* was striking, compared to the other *Chara* species, which had astonishing low amounts. Since pectins are characterized by a high content of GalA, the high amounts of uronic acids in the two pectic fractions in all *Chara* species were not surprising, but again highest in *C. aspera* with 60% in the  $(\text{NH}_4)_2\text{C}_2\text{O}_4$  and 40% in the HCl fraction. As *C. aspera* is the only investigated species which is salt tolerant (Blindow & Schütte, 2007), the involvement of pectins in adaptation to salt water is possible. An increase in pectins in response to this abiotic stress has been shown for several angiosperms (Aquino et al., 2011; Corrêa-Ferreira et al., 2019; Liu et al., 2022). High concentrations of uronic acids were also detected in four other members of the Charophyceae, *Chara corallina*, *C. vulgaris*, *Nitella flexilis* and *N. obtusa* (O'Rourke et al., 2015; Pfeifer et al., 2022; Popper & Fry, 2003) as well as in *Coleochaete scutata* (Coleochaetophyceae). In contrast, the pectic fractions of *S. pratensis* (Zygnematophyceae) contained only low amounts of uronic acids (Pfeifer et al., 2022) and those of two *Klebsormidium* species (Klebsormidiaceae) were completely free of GalA and also GlcA (O'Rourke et al., 2015), thus revealing strong differences in the composition of the pectic fractions of streptophyte cell walls.

Pectins, mainly consisting of non-esterified GalA, have been purified from *Nitella translucens* and *Chara australis* (Anderson & King, 1961a, 1961b). Immunocytochemistry with antibodies directed

against HG (LM19, LM20, JIM5, JIM7, 2F4) supported the presence of this pectic polysaccharide in many members of streptophyte algae (Domozych et al., 2014; Eder & Lütz-Meindl, 2008, 2010; Herburger et al., 2019; Palacio-López et al., 2019; Permman, Herburger, Felhofer, et al., 2021; Permman, Herburger, Niedermeier, et al., 2021; Proseus & Boyer, 2006; Sørensen et al., 2011), but glycan microarray with HG antibodies JIM5 and 2F4 also revealed strong differences. Whereas there was strong reactivity with CDTA extracts of *Chara*, *Coleochaete*, *Cosmarium*, *Penium* and *Netrium*, no reactivity was detected in *Spirogyra*, *Klebsormidium* and *Chlorokybus* (Sørensen et al., 2011). In contradiction to these results, CDTA extracts of *Spirogyra mirabilis* and *Mougeotia disjuncta* showed strong binding, especially to LM19 and JIM5, which both recognize HG with a low degree of esterification (Permman, Herburger, Felhofer, et al., 2021; Permman, Herburger, Niedermeier, et al., 2021). To conclude, it seems that the presence of homogalacturonans is an ancient feature of streptophytes, secondarily lost in some species.

In the presence of RG-I, Rha, Gal and Ara should be detectable in the pectic fractions. Rha accounts for over 10% of the neutral monosaccharides in the  $(\text{NH}_4)_2\text{C}_2\text{O}_4$  fractions of all *Chara* species investigated in this study, Gal (including 3-O-MeGal) is also present in higher amounts, but the content of Ara is low. Low amounts of Ara were also verified for the  $(\text{NH}_4)_2\text{C}_2\text{O}_4$  fractions of *C. vulgaris* and *N. flexilis* (O'Rourke et al., 2015). In *C. australis* and several members of the Zygnematophyceae, linkage-types and antibody reactivities typically associated with Ara and Gal sidechains of RG-I were either absent or present at low levels (Sørensen et al., 2011). Isolation of pectins by oxalate followed by paper chromatography suggested the presence of RG I only in the later-diverging CGA *N. flexilis*, *C. vulgaris* and *C. scutata* (O'Rourke et al., 2015). The antibody LM5 directed against an epitope containing 1,4-linked Gal present in RG-I showed weak binding to CDTA extracts from *Mougeotia disjuncta* and *Spirogyra mirabilis* (Permman, Herburger, Felhofer, et al., 2021; Permman, Herburger, Niedermeier, et al., 2021). To conclude, the presence of RG-I side chains in streptophyte algae is still not finally settled, but is more likely for members of the ZCC grade.

While INRA-RU1 and 2 reactivity (recognition of the RG-I backbone, Ralet et al., 2010) was shown for CDTA extracts of *Mougeotia* and *Spirogyra* (Permman, Herburger, Felhofer, et al., 2021; Permman, Herburger, Niedermeier, et al., 2021), our  $(\text{NH}_4)_2\text{C}_2\text{O}_4$  fractions showed no binding (Figure S3) in any of the *Chara* species investigated. This hints to the absence of RG-I, at least in this genus of the Charophyceae.

A special feature of all pectic fractions of the four *Chara* species was 3-O-MeGal, which was also detected in *C. vulgaris* and *C. corallina* (Sørensen et al., 2011). It has been suggested that this methylated monosaccharide might have replaced Ara in RG-I of *Chara* species (O'Rourke et al., 2015), which is contradictory to our results that propose the absence of RG-I in *Chara* species.

Investigations on glycosyl linkages revealed none of the characteristic sugars of RG II (2-OMeFuc, 2-OMeXyl, apiose, aceric acid) in streptophyte algae (Sørensen et al., 2011). This is in line with several other publications proposing RG-II as a typical land plant feature (Matsunaga

et al., 2004; Mikkelsen et al., 2014). Therefore, further investigations are also necessary to clarify the evolutionary roots of RG-II.

### 4.3 | Ancestral hemicellulose core structures seem to have diversified after the divergence of Charales and all other streptophytes

Since most hemicelluloses can be extracted under alkaline conditions (Scheller & Ulvskov, 2010), two alkaline fractions (sodium carbonate and KOH) were extracted from the cell walls of the four investigated *Chara* species. Xyl, Man, and Glc were abundant in the hemicellulose fractions of all *Chara* spp., which might be part of xylans, xyloglucans and (gluco)mannans. Striking was the low Xyl content of the KOH fraction of *C. aspera*. This is also demonstrated by the Xyl:Glc ratio. In the other *Chara* species, this ranges from 1.3 to 1.7:1, whereas *C. aspera* shows a ratio of 1:4.6. Presence of xylans and xyloglucans in the cell walls of *C. globularis*, *C. subspinosa* and *C. tomentosa* was supported by ELISA with LM10 (xylans) and LM15 (xyloglucans). As the KOH fraction of *C. aspera* showed no reactivity with the antibodies, this species might be characterized by a lack, or structural modifications, of both hemicelluloses. It has to be mentioned that LM10 only detects not or only slightly substituted xylans (McCartney et al., 2005). Interestingly, the NaOH extract of *C. corallina* also showed no binding to LM10, but bound to LM11 detecting arabinoxylans as well (Sørensen et al., 2011).

In general, there is good evidence for the presence of xylans and xyloglucans in streptophyte algae. This is based on investigations with antibodies directed against xylan and xyloglucan epitopes (Domozych et al., 2009; Eder & Lütz-Meindl, 2008; Ikegaya et al., 2012; Mikkelsen et al., 2021; Permann, Herburger, Felhofer, et al., 2021; Permann, Herburger, Niedermeier, et al., 2021; Sørensen et al., 2011), but also on structural characterization (Ikegaya et al., 2008; Mikkelsen et al., 2021; Sørensen et al., 2011) and investigations of enzymes involved in the biosynthesis (Del Bem & Vincentz, 2010; Franková & Fry, 2021; Mikkelsen et al., 2014; Mikkelsen et al., 2021; Nishiyama et al., 2018).

The presence of fucosylated and galactosylated xyloglucans has been shown for *Mesotaenium* (Mikkelsen et al., 2021), underlining that these xyloglucan substitutions known from land plants are also present, at least in some, streptophyte algae. Especially in the sodium carbonate fractions of the *Chara* species investigated here, Gal and Fuc are present in amounts between 2.8% and 9.8%, maybe indicating fucosylated and/or galactosylated xyloglucans.

As far as mannans are concerned, there are convincing data suggesting the presence in most, if not all, charophyte algae. These data range from results of chemical analysis of cell wall fractions of *Chara* and *Nitella* (O'Rourke et al., 2015) to antibody profiling results (Domozych et al., 2009; Sørensen et al., 2011). Our chemical analysis is in support of this conclusion for *Chara* and *Nitellopsis* species by showing relevant amounts of Man in the hemicellulosic and pectic fractions (Figure 1A). This is in line with the

composition data for *Klebsormidium* spp., which also showed widespread occurrence of Man in the different cell wall fractions (O'Rourke et al., 2015). Mannan structures, in general, have to be further investigated for defining the occurrence as homo- or heteromannan, as this is currently unknown for all charophyte algae (Franková & Fry, 2021). Most interestingly, *Chara*, *Nitella* and *Klebsormidium* have been demonstrated to contain unusually high trans- $\beta$ -mannanase and trans- $\beta$ -xylanase activities. These have been proposed as hemicellulose remodelling strategies alternative to xyloglucan endotransglucosylase (XET) activity known from land plants (Franková & Fry, 2021).

### 4.4 | Purified aqueous extracts include unusual rhamnans and galactans

#### 4.4.1 | Gel diffusion assay

Detection of AGPs is possible by precipitation with  $\beta$ GlcY (Yariv et al., 1962). Although the exact precipitation mechanism has not yet been precisely determined, it is certain that a  $\beta$ -1,3-linked galactan is important for this interaction (Kitazawa et al., 2013; Paulsen et al., 2014). In addition, it has been proposed that high concentrations of 1,6-linked galactans can interfere with the precipitation, either directly by steric hindrance (Kiyohara et al., 1989) or relatively by a shifted 1,6-Gal to 1,3-Gal ratio (Kitazawa et al., 2013; Paulsen et al., 2014).

In a radial gel diffusion assay with  $\beta$ GlcY of AE from all *Chara* species showed no precipitation lines, proposing the absence of AGPs in this genus. After purification of AE by treatment with  $\alpha$ -amylase and pectinase (AE\_AP; deletion of starch and homogalacturonan, which might have been coextracted), thin precipitation lines could be detected (Figure S3), possibly originating from 1,3-linked galactans and not from AGPs, as no Hyp was present (see below).

#### 4.4.2 | Analyses of the carbohydrate moiety

Seed plant, fern and bryophyte AGPs have been isolated from aqueous extracts (AE) rich in Ara and Gal by precipitation with  $\beta$ GlcY (Bartels & Classen, 2017; Classen et al., 2004; Happ & Classen, 2019; Mueller et al., 2023). The AE fraction compositions of the cell walls of the investigated *Chara* species differed with high Gal contents but only low amounts of Ara. AE of *Nitellopsis* was slightly different with higher amounts of Rha and Ara. AE of *C. aspera* was striking due to the high content of uronic acids (over 30%). Furthermore, the presence of 3-O-MeGal was striking in all AE, especially in *C. aspera*. Methylation of one hydroxyl-group of monosaccharides is a rare modification of different carbohydrates and has been described for some bacteria, fungi, worms, molluscs and also plants (for review see Staudacher, 2012). It offers the possibility to modulate glycan structures, thereby leading to new biological activities. In plants, galactose is the most common methylated

hexose (Staudacher, 2012), especially in algae. 4-O-MeGal and 3-O-MeGal occur in red algae (Allsobrook et al., 1974; Araki et al., 1986; Navarro & Stortz, 2008). In cell walls of chlorophyte green algae, polysaccharides containing 3-O-MeGal, 2-O-MeRha and 3-O-MeRha (*Chlorella vulgaris*) or 3-O-MeRha and 3-O-MeFuc (*Botryococcus braunii*) were found (Allard & Casadevall, 1990; Ogawa et al., 1994; Ogawa et al., 1997). For *Chlorella vulgaris*, it was shown that 3-O-MeGal is part of a neutral galactan with a ratio of Gal: 3-O-MeGal of 7.1:1 (Ogawa et al., 2001). In *S. pratensis*, 3-O-MeGal, 2-O-MeRha and 3-O-MeRha were detected only in trace amounts (Pfeifer et al., 2022). In the streptophyte algae *K. flaccidum*, *C. corallina* and *C. scutate*, 3-O-MeRha was also identified in small amounts (Popper & Fry, 2003), but 3-O-MeGal was not detected at all (Popper et al., 2001). More recently, it was shown that pectins of *C. vulgaris* are characterized by the presence of 3-O-MeGal (O'Rourke et al., 2015). Among the land plants, the cell walls of bryophytes and ferns contain 3-O-MeRha, especially as part of AGPs (Bartels et al., 2017; Bartels & Classen, 2017; Baumann et al., 2021; Happ & Classen, 2019; Mueller et al., 2023), or RG-II (Matsunaga et al., 2004), whereas higher concentrations of 3-O-MeGal were detected in the cell walls of the young leaves of both homosporous (*Lycopodium*, *Huperzia* and *Diphasiastrum*) and heterosporous (*Selaginella*) lycophytes (Popper et al., 2001). Although only rarely, 3-O-MeGal was found in some seed plant polysaccharides as well (Barsett & Paulsen, 1992; Hokputsa et al., 2004), even as part of an arabinogalactan-protein (Capek, 2008).

To verify the presence of arabinogalactans, antibodies directed against arabinogalactan epitopes present in AGPs are commonly used (e.g., JIM8, JIM13, JIM16, LM2, LM6, LM14, KM1, MAC207). AE of all *Chara* species investigated showed comparable binding profiles in ELISA with JIM13, LM2, LM6 and KM1. There was nearly

no binding of *Chara* AE to LM6, indicating lack of detectable 1,5-linked Ara. In contrast, AE of *N. obtusa* bound to LM6 and structure elucidation revealed high amounts of 1,5-linked Ara (Table 3). KM1, which recognizes 1,6-linked Gal, bound to AE of all *Chara* species and also to AE of *N. obtusa* (Pfeifer et al., 2022) thus revealing presence of 1,6-linked Gal. Binding of AE to JIM13 with an epitope probably including Rha and uronic acids was comparable for the *Chara* species but very low for *N. obtusa* (Pfeifer et al., 2022). In ELISA with LM2, *C. aspera* reacted very strongly. According to Ruprecht et al. (2017), this antibody recognizes (1 → 6)-β-D-Galp units with terminal β-D-GlcAp. Probably the high content of 1,6-Gal residues in AE of *C. aspera* is responsible for the higher affinity to this antibody. In ELISA experiments with AE of *S. pratensis* (Pfeifer et al., 2022), no affinity was detected for LM6 and KM1, whereas there was strong binding to JIM13. CDTA extracts of other members of the Zygnematophyceae (*S. mirabilis* and *Mougeotia* sp.) also showed strong interaction with JIM13 (Permann, Herburger, Felhofer, et al., 2021; Permann, Herburger, Niedermeier, et al., 2021). In a glycan microarray, different antibodies directed against AG epitopes (LM2, LM14, JIM8, JIM13 and MAC207) have been tested for interaction with different streptophyte algae (Sørensen et al., 2011). All antibodies (except for LM2) and especially JIM13 bound to CDTA extracts of *C. corallina*, but JIM13 was the only antibody binding to *Spirogyra* CDTA extracts, thus hinting at strong structural differences between the Charophyceae and Zygnematophyceae. Several members of the Zygnematophyceae showed positive interaction with JIM13 (Domozych et al., 2009; Eder et al., 2008; Palacio-López et al., 2019; Ruiz-May et al., 2018). Interestingly, *K. flaccidum*, representing the lower-branching KCM-grade, showed no reactivity with antibodies directed against arabinogalactan epitopes (Sørensen et al., 2011; Steiner et al., 2020).

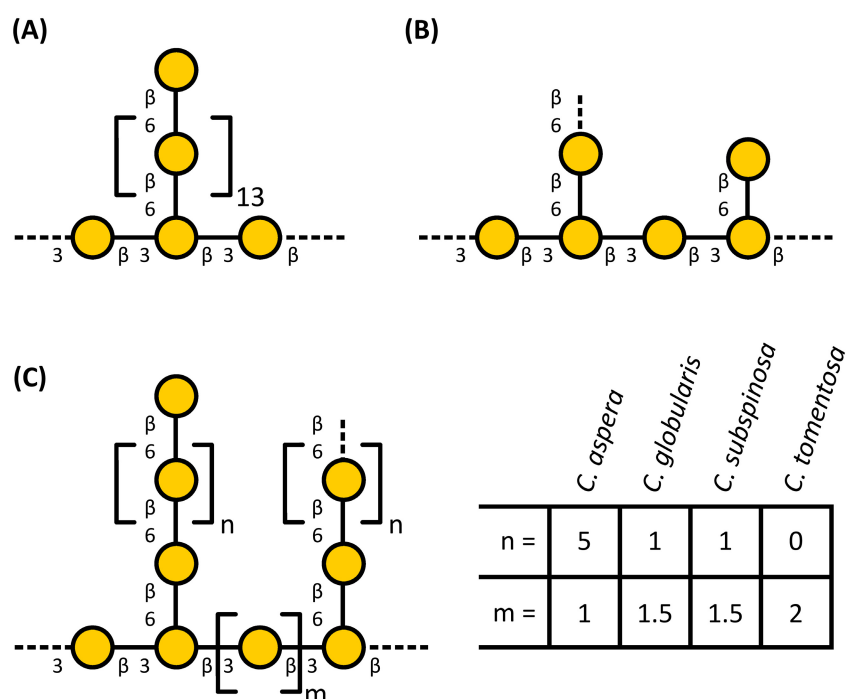


**FIGURE 4** Partial structural proposals for galactans of *Chara* species in the context of other algal galactan structures. (A) Structural proposal of *Chlorella vulgaris* based on the published results of Ogawa et al. (2001). Patterns of methylation are not shown. (B) Galactan structures of *Nitellopsis obtusa*. (C) Galactan structures of the investigated four *Chara* species. The structural features were inferred from the linkage-type analysis. The dashed lines symbolize attachment sites for galactoses (main chain) or for other monosaccharides (side chain). Part of the Gal residues are methylated (see Table 2 for amounts of 3-O-MeGal).

Structural analyses verified the presence of unusual galactans (Figure 4). Galactan linkage-types typical for AGPs were present. These were detected by antibodies directed against AGPs (see above) and weak interaction with Yariv's reagent (Kitazawa et al., 2013; Paulsen et al., 2014). A special feature were high amounts of 3-O-MeGal, present in 1,6-linkage or as terminal residue. The ratio of Gal to 3-O-MeGal varied (see Table 2) and was highest for *C. aspera* (1:1.2). There was a shifted in the ratio of backbone galactan to side-chain galactans between the species. *C. aspera* shows the longest 1,6-Gal side chains, whereas *N. obtusa* is special due to short 1,6-linked Gal side chains. Similar galactan structures (longer 1,6-linked Gal side chains; lower degree of methylated Gal) have been isolated from *Chlorella vulgaris*, a unicellular member of the Chlorophyta (Ogawa et al., 2001), hinting at a shared evolutionary origin.

Another interesting finding of linkage-type analysis were high amounts of 1,4-linked Rhap in all investigated members of the Charales. To the best of our knowledge, no plant polysaccharide with a substantial amount of 1,4-linked Rhap has been described up to now. Typical linkage types known for Rha in seed plants are 1,2- and 1,2,4-linked Rha residues as part of RG-I. A main component of the fibers extracted from the green algae *Monostroma angicava* and *Monostroma nitidum* (Chlorophyceae) are sulfated rhamnans with 1,3- and 1,2-linked Rha residues (Liu et al., 2018; Suzuki & Terasawa, 2020) and the rhamnagalactan-protein isolated from *Spirogyra pratensis* is rich in 1,3-linked Rhap (Pfeifer et al., 2022).

#### 4.4.3 | Hydroxyproline seems to be absent in Charales and AGP-associated P4H activity is questionable

The protein backbone of classical AGPs consists of an N-terminal signal peptide, a protein sequence rich in proline (Pro), alanine (Ala), serine (Ser), and threonine (Thr; PAST), and a C-terminal domain (Johnson et al., 2018). The carbohydrate moieties are covalently linked to the protein part via Hyp. Hydroxylation of Pro to Hyp is catalyzed by the enzyme P4H (Seifert et al., 2021).

In different studies, the occurrence of Hyp was tested in various chlorophyte algae and the charophyte algae *S. pratensis*, *Nitella* sp. and *N. obtusa*. Hyp was detected in all algae, except of the two algae genera of the Charophyceae family: *Nitella* and *Nitellopsis* (Gotelli & Cleland, 1968; Morrison et al., 1993; Pfeifer et al., 2022; Thompson & Preston, 1967). Our results that Hyp is missing in all investigated *Chara* species is in support of these previous results and fosters the assumption that Hyp is absent in all members of the Charophyceae.

At the first glimpse, the finding of seven P4H homologs via BLAST analysis is in contrast to this statement. With the here presented analysis of the relevant amino acids in both catalytic sites (compare Hieta & Myllyharju, 2002; Keskiäho et al., 2007; Koski et al., 2007; Koski et al., 2009) it is likely that most homologs lost their functionality for prolyl-hydroxylation either in general or with regard to the characteristic HRGP substrates. The substrate

specificity is highly dependent on the substrate tunnel being shaped by the  $\beta$ 3- $\beta$ 4 loop as well as the  $\beta$ II- $\beta$ III loop, which cover the tripeptide structure of the substrate. In direct comparison with various human P4H  $\alpha$ -subunits (C-P4HI-III and HIF-P4H-2), it was shown that both regions have a certain degree of flexibility (Koski et al., 2009). Numerous studies with recombinant enzyme expression underlined the flexibility in utilized substrates (Mócsai et al., 2021; Velasquez et al., 2015; Vlad et al., 2010). Despite of the described activities of P4Hs on different substrates, it is not possible to predict specificity conclusively (see Moussu & Ingram, 2023). The few studies comparing substrate activities (Mócsai et al., 2021; Velasquez et al., 2015; Vlad et al., 2010) have included an AGP peptide in their analyses but also reveal that for *C. reinhardtii* P4H this activity was not determined (Vlad et al., 2010). The selected candidate sequence GBG85197 from *C. braunii* showed overall similarity to the two P4Hs from *A. thaliana* and *C. reinhardtii* (Figure 3) with various structural variations in the two flexible regions. Even though the catalytically relevant amino acids are present (Hieta & Myllyharju, 2002; Keskiäho et al., 2007; Koski et al., 2007; Koski et al., 2009), this could mean extremely different or even lacking activity. Timmins et al. (2017) performed excessive mutations (Y140F, Y140G, W243F, W243G, Y140G/W243G) in the two investigated loops and showed inactivity, changed regioselectivity or different substrate activity by mutation of single amino acids. Presence of a putatively functional P4H and lack of hydroxyproline in the biochemical assays is explainable in different ways: (1) The occurrence of the coding gene in the genome is not equivalent to permanent expression of a functional protein. This could be occasionally expressed or not expressed following a distinct (environmental) stimulus. (2) The P4H coding gene could be a remnant of the least common ancestor of all Chloroplastida, which utilized the enzyme for hydroxylation of very specialized substrates. Exemplarily, the cell walls in Chlamydomonales are formed nearly exclusively by (glyco-) proteins showing O-glycosylation (Bollig et al., 2007; Ferris et al., 2001; Miller et al., 1972; Voigt et al., 2014; Woessner & Goodenough, 1994). Whether their glycosylation, showing similarities to land plant extensins (Bollig et al., 2007), is performed (similar to embryophytes) by homologs of carbohydrate-active enzymes from the GT95, GT77 and GT47 families is questionable by looking at the work of Barolo et al. (2020) who detected few, if any, homologs in microalgal genomes. (3) The complex interplay of three different P4Hs (AtP4H2, AtP4H5 and AtP4H13) was shown in *A. thaliana* (Velasquez et al., 2015). The formation of homodimers of AtP4H5 or heterodimers of AtP4H5 with either AtP4H2 or AtP4H13 is required for correct peptidyl-proline hydroxylation. This is the case for at least extensins, but cannot be ruled out for other HRGPs. From these three P4Hs, GBG85197 showed most similarity with AtP4H13 in the  $\beta$ II- $\beta$ III loop thus hinting potential inactivity in a monomeric state. All these three possible explanations are speculative but highlight the general aim that presence or absence of P4H homologs should not be seen equivalent to presence or absence of AGPs or extensins. The latter has to be individually shown by a combination with analytical methods as shown in this study.

## 5 | CONCLUSION

Although presence of pectic polysaccharides is unquestionable and especially the cell walls of *C. aspera* contain huge amounts of these polysaccharides possibly involved in salt tolerance of this species, further investigations have to follow to elucidate the exact structural composition and to clarify whether only homogalacturonan or also RG-I or even RG-II have evolutionary roots in algae. The most prominent unusual structural features detected in the aqueous extracts of the investigated Charales were 1,4-linked rhamnans and 1,3-, 1,6- and 1,3,6-linked partially methylated galactans. However, these galactans were not part of AGPs. Although one possible functional sequence of P4H was detected in the genome of *C. braunii*, no Hyp (necessary for linkage of the galactan to the protein moiety in AGPs) was detected in any of the investigated species. The fact that antibodies directed against AGP epitopes showed cross reactivities with the unusual methylated galactans is a reminder that results only based on antibodies are not always reliable. Our work reveals strong differences of the cell walls of members of the Charophyceae compared to those of seed plants and even to those of the other members of the higher-branching ZCC-grade of streptophyte algae, namely the Coleochaetophyceae and the Zygnematophyceae. More detailed investigations of the cell walls of the different streptophyte algal taxa are necessary to understand how these algae met the challenge of cell wall adaptation necessary for life on land.

### AUTHOR CONTRIBUTIONS

Birgit Classen and Lukas Pfeifer planned and designed the research. Hendrik Schubert collected and identified the plant material. Felicitas Erdt, Kim-Kristine Mueller, Lukas Pfeifer and Jon Utermöhlen performed the extractions as well as carbohydrate and ELISA experiments. Jean Bastian Just Zehge performed preliminary analytical work on *Chara* species from Austria. Lukas Pfeifer performed bioinformatic searches. Lukas Pfeifer and Kim-Kristine Mueller created all main text figures. All authors analysed the data (Birgit Classen, Felicitas Erdt, Kim-Kristine Mueller, Lukas Pfeifer: carbohydrate analysis; Lukas Pfeifer bioinformatics search for P4Hs). Birgit Classen, Kim-Kristine Mueller and Lukas Pfeifer wrote the draft manuscript; all authors revised the manuscript, read and approved the final manuscript.

### ACKNOWLEDGMENTS

The authors thank Prof. Dr. Michael Schagerl and Barbara Mähner from the Department for Limnology and Oceanography of the University of Wien for collection of *Chara* species used in preliminary experiments. Open Access funding enabled and organized by Projekt DEAL.

### FUNDING INFORMATION

LP and BC (project-number 440046237) are grateful for funding within the framework of MAdLand (<http://madland.science>), priority programme 2237 of the German Research Foundation (DFG). HS also thanks the DFG for funding (project SCHU 983/23-1).

### DATA AVAILABILITY STATEMENT

All relevant data can be found within the manuscript and its supporting materials.

### ORCID

Lukas Pfeifer  <https://orcid.org/0000-0002-7076-4597>

Birgit Classen  <https://orcid.org/0000-0003-1452-801X>

### REFERENCES

- Allard, B. & Casadevall, E. (1990) Carbohydrate composition and characterization of sugars from the green microalga *Botryococcus braunii*. *Phytochemistry*, 29, 1875–1878.
- Allsbrook, A.J.R., Nunn, J.R. & Parolis, H. (1974) The linkage of 4-O-methyl-L-galactose in the sulphated polysaccharide of *Aeodes ulvoidea*. *Carbohydrate Research*, 36, 139–145.
- Anderson, D.M. & King, N.J. (1961a) Polysaccharides of the Characeae. II. The carbohydrate content of *Nitella translucens*. *Biochimica et Biophysica Acta*, 52, 441–449.
- Anderson, D.M. & King, N.J. (1961b) Polysaccharides of the Characeae. III. The carbohydrate content of *Chara australis*. *Biochimica et Biophysica Acta*, 52, 449–454.
- Aquino, R.S., Grativol, C. & Mourão, P.A.S. (2011) Rising from the Sea: correlations between sulfated polysaccharides and salinity in plants. *PLoS One*, 6, e18862.
- Araki, S., Satake, M., Ando, S., Hayashi, A. & Fujii, N. (1986) Characterization of a diphosphonopentaosylceramide containing 3-O-methylgalactose from the skin of *Aplysia kurodai* (sea hare). *Journal of Biological Chemistry*, 261, 5138–5144.
- Barolo, L., Abbriano, R.A., Commault, A.S., George, J., Kahlke, T., Fabris, M. et al. (2020) Perspectives for glyco-engineering of recombinant biopharmaceuticals from microalgae. *Cell*, 9, 633.
- Barsett, H. & Paulsen, B.S. (1992) Separation, isolation and characterization of acidic polysaccharides from the inner bark of *Ulmus glabra* Huds. *Carbohydrate Polymers*, 17, 137–144.
- Bartels, D., Baumann, A., Maeder, M., Geske, T., Heise, E.M., von Schwartzberg, K. et al. (2017) Evolution of plant cell wall: Arabinogalactan-proteins from three moss genera show structural differences compared to seed plants. *Carbohydrate Polymers*, 163, 227–235.
- Bartels, D. & Classen, B. (2017) Structural investigations on arabinogalactan-proteins from a lycophyte and different monilophytes (ferns) in the evolutionary context. *Carbohydrate Polymers*, 172, 342–351.
- Baumann, A., Pfeifer, L. & Classen, B. (2021) Arabinogalactan-proteins from non-coniferous gymnosperms have unusual structural features. *Carbohydrate Polymers*, 261, 11783.
- Blakeney, A.B., Harris, P.J., Henry, R.J. & Stone, B.A. (1983) A simple and rapid preparation of alditol acetates for monosaccharide analysis. *Carbohydrate Research*, 113, 291–299.
- Blindow, I. & Schütte, M. (2007) Elongation and mat formation of *Chara aspera* under different light and salinity conditions. *Hydrobiologia*, 584, 69–76.
- Blumenkrantz, N. & Asboe-Hansen, G. (1973) New method for quantitative determination of uronic acids. *Analytical Biochemistry*, 34, 484–489.
- Bollig, K., Lamshöft, M., Schweimer, K., Marner, F.-J., Budzikiewicz, H. & Waffenschmidt, S. (2007) Structural analysis of linear hydroxyproline-bound O-glycans of *Chlamydomonas reinhardtii*—conservation of the inner core in *Chlamydomonas* and land plants. *Carbohydrate Research*, 342, 2557–2566.
- Bowman, J.L. (2022) The origin of a land flora. *Nature Plants*, 8, 1352–1369.
- Capek, P. (2008) An arabinogalactan containing 3-O-methyl-D-galactose residues isolated from the aerial parts of *Salvia officinalis* L. *Carbohydrate Research*, 343, 1390–1393.

- Clarke, A.E., Gleeson, P.A., Jermyn, M.A. & Knox, R.B. (1978) Characterization and localization of  $\beta$ -lectins in lower and higher plants. *Australian Journal of Plant Physiology*, 5, 707–722.
- Classen, B., Csavas, M., Borbas, A., Dingermann, T. & Zundorf, I. (2004) Monoclonal antibodies against an arabinogalactan-protein from pressed juice of *Echinacea purpurea*. *Planta Medica*, 70, 861–865.
- Correa-Ferreira, M.L., Viudes, E.B., de Magalhaes, P.M., de Santana Filho, A.P., Sasaki, G.L., Pacheco, A.C. et al. (2019) Changes in the composition and structure of cell wall polysaccharides from *Artemisia annua* in response to salt stress. *Carbohydrate Research*, 483, 107753.
- de Vries, J. & Archibald, J.M. (2018) Plant evolution: landmarks on the path to terrestrial life. *New Phytologist*, 217, 1428–1434.
- Del Bem, L.E.V. & Vincenz, M.G.A. (2010) Evolution of xyloglucan-related genes in green plants. *BMC Evolutionary Biology*, 10, 341.
- DiTomaso, J.M., Kyser, G.B., Oneto, S.R., Wilson, R.G., Orloff, S.B., Anderson, L.W. et al. (2013) *Weed control in natural areas in the western United States*. Davies, CA: Weed Research and Information Center, University of California, p. 544.
- Domozych, D.S. & Bagdan, K. (2022) The cell biology of charophytes: exploring the past and models for the future. *Plant Physiology*, 190, 1588–1608.
- Domozych, D.S., Sørensen, I., Sacks, C., Brechka, H., Andreas, A., Fangel, J.U. et al. (2014) Disruption of the microtubule network alters cellulose deposition and causes major changes in pectin distribution in the cell wall of the green alga, *Penium margaritaceum*. *Journal of Experimental Botany*, 65, 465–479.
- Domozych, D.S., Sørensen, I. & Willats, W.G.T. (2009) The distribution of cell wall polymers during antheridium development and spermatogenesis in the Charophycean green alga, *Chara corallina*. *Annals of Botany*, 104, 1045–1056.
- Eder, M. & Lütz-Meindl, U. (2008) Pectin-like carbohydrates in the green alga *Micrasterias* characterized by cytochemical analysis and energy filtering TEM. *Journal of Microscopy*, 231, 201–214.
- Eder, M. & Lütz-Meindl, U. (2010) Analyses and localization of pectin-like carbohydrates in cell wall and mucilage of the green alga *Netrium digitus*. *Protoplasma*, 243, 25–38.
- Eder, M., Tenhaken, R., Driouich, A. & Lütz-Meindl, U. (2008) Occurrence and characterization of arabinogalactan-like proteins and hemicelluloses in *Micrasterias* (Streptophyta). *Journal of Phycology*, 44, 1221–1234.
- Estevez, J.M., Fernández, P.V., Kasulin, L., Dupree, P. & Ciancia, M. (2009) Chemical and in situ characterization of macromolecular components of the cell walls from the green seaweed *Codium fragile*. *Glycobiology*, 19, 212–228.
- Estevez, J.M., Leonardi, P.I. & Alberghina, J.S. (2008) Cell wall carbohydrate epitopes in the green alga *Oedogonium bharuchae* f. *minor* (Oedogoniales, Chlorophyta). *Journal of Phycology*, 44, 1257–1268.
- Ferris, P.J., Woessner, J.P., Waffenschmidt, S., Kilz, S., Drees, J. & Goodenough, U.W. (2001) Glycosylated polyproline II rods with kinks as a structural motif in plant hydroxyproline-rich glycoproteins. *Biochemistry*, 40, 2978–2987.
- Franková, L. & Fry, S.C. (2021) Hemicellulose-remodelling transglycanase activities from charophytes: towards the evolution of the land-plant cell wall. *The Plant Journal*, 108, 7–28.
- Fu, H., Yadav, M.P. & Nothnagel, E.A. (2007) *Physcomitrella patens* arabinogalactan proteins contain abundant terminal 3-O-methyl-L-rhamnosyl residues not found in angiosperms. *Planta*, 226, 1511–1524.
- Gotelli, I.B. & Cleland, R. (1968) Differences in the occurrence and distribution of hydroxyproline-proteins among the algae. *American Journal of Botany*, 55, 907–914.
- Hahsler, M. & Nagar, A. (2019) *rBLAST: R Interface for the basic local alignment search tool. R package version 0.99.2*. Available from: <https://github.com/mhahsler/rBLAST>
- Happ, K. & Classen, B. (2019) Arabinogalactan-proteins from the liverwort *Marchantia polymorpha* L., a member of a basal land plant lineage, are structurally different to those of angiosperm. *Plants*, 8, 460.
- Harholt, J., Moestrup, Ø. & Ulvskov, P. (2016) Why plants were terrestrial from the beginning. *Trends in Plant Science*, 21, 96–101.
- Harris, P.J., Henry, R.J., Blakeney, A.B. & Stone, B.A. (1984) An improved procedure for the methylation analysis of oligosaccharides and polysaccharides. *Carbohydrate Research*, 127, 59–73.
- Herburger, K., Xin, A. & Holzinger, A. (2019) Homogalacturonan accumulation in cell walls of the green alga *Zygnema* sp. (Charophyta) increases desiccation resistance. *Frontiers in Plant Science*, 10, 540.
- Hervé, C., Siméon, A., Jam, M., Cassin, A., Johnson, K.L., Salmeán, A.A. et al. (2016) Arabinogalactan proteins have deep roots in eukaryotes: identification of genes and epitopes in brown algae and their role in *Fucus serratus* embryo development. *New Phytologist*, 209, 1428–1441.
- Hess, S., Williams, S.K., Busch, A., Irisarri, I., Delwiche, C.F., de Vries, S. et al. (2022) A phylogenomically informed five-order system for the closest relatives of land plants. *Current Biology*, 20, 4473–4482.e7.
- Hieta, R. & Myllyharju, J. (2002) Cloning and characterization of a low molecular weight prolyl 4-hydroxylase from *Arabidopsis thaliana*. *The Journal of Biological Chemistry*, 277, 23965–23971.
- Hokputsa, S., Harding, S.E., Inngjerdigen, K., Jumel, K., Michaelsen, T.E., Heinze, T. et al. (2004) Bioactive polysaccharides from the stems of the thai medicinal plant *Acanthus ebracteatus*: their chemical and physical features. *Carbohydrate Research*, 339, 753–762.
- Ikegaya, H., Hayashi, T., Kaku, T., Iwata, K., Sonobe, S. & Shimmen, T. (2008) Presence of xyloglucan-like polysaccharide in *Spirogyra* and possible involvement in cell-cell attachment. *Phycological Research*, 56, 216–222.
- Ikegaya, H., Nakase, T., Iwata, K., Tsuchida, H., Sonobe, S. & Shimmen, T. (2012) Studies on conjugation of *Spirogyra* using monoclonal culture. *Journal of Plant Research*, 125, 457–464.
- Johnson, K.L., Cassin, A.M., Lonsdale, A., Ka-Shu Wong, G., Soltis, D.E., Miles, N.W. et al. (2017) Insights into the evolution of hydroxyproline-rich glycoproteins from 1000 plant transcriptomes. *Plant Physiology*, 174, 904–921.
- Johnson, K.L., Jones, B.J., Schultz, C.J. & Bacic, A. (2018) Non-enzymic cell wall (glyco)proteins. In: Roberts, J.A. (Ed.) *Annual plant reviews online*. Hoboken, NJ: John Wiley & Sons Ltd. Available from: <https://doi.org/10.1002/9781119312994.apr0070>
- Katoh, K. & Standley, D.M. (2013) MAFFT multiple sequence alignment software version 7: improvements in performance and usability. *Molecular Biology and Evolution*, 30, 772–780.
- Keskiaho, K., Hieta, M., Sormunen, R. & Myllyharju, J. (2007) *Chlamydomonas reinhardtii* has multiple prolyl 4-hydroxylases, one of which is essential for proper cell wall assembly. *The Plant Cell*, 19, 256–269.
- Kitazawa, K., Tryfona, T., Yoshimi, Y., Hayashi, Y., Kawachi, S., Antonov, L. et al. (2013)  $\beta$ -galactosyl Yariv reagent binds to the  $\beta$ -1,3-galactan of arabinogalactan proteins. *Plant Physiology*, 161, 1117–1126.
- Kiyohara, H., Cyong, J.-C. & Yamada, H. (1989) Relationship between structure and activity of an anticomplementary arabinogalactan from the roots of *Angelica acutiloba* kitagawa. *Carbohydrate Research*, 193, 193–200.
- Koski, M.K., Hieta, M., Böllner, C., Kivirikko, K.I., Myllyharju, J. & Wierenga, R.K. (2007) The active site of an algal prolyl 4-hydroxylase has a large structural plasticity. *The Journal of Biological Chemistry*, 282, 37112–37123.
- Koski, M.K., Hieta, M., Rönkä, A., Myllyharju, J. & Wierenga, R.K. (2009) The crystal structure of an algal prolyl 4-hydroxylase complexed with a proline-rich peptide reveals a novel buried tripeptide binding motif. *The Journal of Biological Chemistry*, 284, 25290–25301.
- Lampert, D.T.A. (2023) The growth oscillator and plant stomata: an open and shut case. *Plants*, 12, 2531.

- Lampert, D.T.A. & Várnai, P. (2013) Periplasmic arabinogalactan glycoproteins act as a calcium capacitor that regulates plant growth and development. *New Phytologist*, 197, 58–64.
- Leebens-Mack, J.H., Barker, M.S., Carpenter, E.J., Deyholos, M.K., Gitzendanner, M.A., Graham, S.W. et al. (2019) One thousand plant transcriptomes and the phylogenomics of green plants. *Nature*, 574, 679–685.
- Leszczuk, A., Kalaitzis, P., Kulik, J. & Zdunek, A. (2023) Review: structure and modifications of arabinogalactan proteins (AGPs). *BMC Plant Biology*, 23, 45.
- Liu, J., Shao, Y., Feng, X., Otie, V., Matsuura, A., Irshad, M. et al. (2022) Cell wall components and extensibility regulate root growth in *Sueda salsa* and *Spinacia oleracea* under salinity. *Plants*, 11, 900.
- Liu, X., Wang, S., Cao, S., He, X., Qin, L., He, M. et al. (2018) Structural characteristics and anticoagulant property in vitro and in vivo of a seaweed sulfated rhamnan. *Marine Drugs*, 16, 243.
- Ma, Y., Zeng, W., Bacic, A. & Johnson, K. (2018) AGPs through time and space. In: Roberts, J.A. (Ed.) *Annual plant reviews online*. Hoboken, NJ: John Wiley & Sons Ltd. Available from: <https://doi.org/10.1002/9781119312994.apr0608>
- Marcus, S.E., Verherbruggen, Y., Hervé, C., Ordaz-Ortiz, J.J., Farkas, V., Pedersen, H.L. et al. (2008) Pectic homogalacturonan masks abundant sets of xyloglucan epitopes in plant cell walls. *BMC Plant Biology*, 8, 60.
- Mareri, L., Romi, M. & Cai, G. (2018) Arabinogalactan proteins: actors or spectators during abiotic and biotic stress in plants? *Plant Biosystems*, 153, 173–185.
- Matsunaga, T., Ishii, T., Matsumoto, S., Higuchi, M., Darvill, A., Albersheim, P. et al. (2004) Occurrence of the primary cell wall polysaccharide rhamnogalacturonan II in pteridophytes, lycophytes, and bryophytes. Implications for the evolution of vascular plants. *Plant Physiology*, 134, 339–351.
- McCartney, L., Marcus, S.E. & Knox, J.P. (2005) Monoclonal antibodies to plant cell wall xylans and arabinoxylans. *Journal of Histochemistry & Cytochemistry*, 53, 543–546.
- Mikkelsen, M.D., Harholt, J., Ulvskov, P., Johansen, I.E., Fangel, J.U., Doblin, M.S. et al. (2014) Evidence for land plant cell wall biosynthetic mechanisms in charophyte green algae. *Annals of Botany*, 114, 1217–1236.
- Mikkelsen, M.D., Harholt, J., Westereng, B., Domozych, D., Fry, S.C., Johansen, I.E. et al. (2021) Ancient origin of fucosylated xyloglucan in charophycean green algae. *Communications Biology*, 4, 754.
- Miller, D.H., Lampert, D.T.A. & Miller, M. (1972) Hydroxyproline heterooligosaccharides in *Chlamydomonas*. *Science*, 176, 918–920.
- Mócsai, R., Göritzer, K., Stenitzer, D., Maresch, D., Strasser, R. & Altmann, F. (2021) Prolyl hydroxylase paralogs in *Nicotiana benthamiana* show high similarity with regard to substrate specificity. *Frontiers in Plant Science*, 12, 63659.
- Morrison, J.C., Greve, L.C. & Richmond, P.A. (1993) Cell wall synthesis during growth and maturation of *Nitella internodal* cells. *Planta*, 189, 321–328.
- Moussu, S. & Ingram, G. (2023) The EXTENSIN enigma. *The Cell Surface*, 9, 100094.
- Mueller, K.-K., Pfeifer, L., Schuldt, L., Szóvényi, P., de Vries, S., de Vries, J. et al. (2023) Fern cell walls and the evolution of arabinogalactan proteins in streptophytes. *The Plant Journal*, 114, 875–894. Available from: <https://doi.org/10.1111/tj.16178>
- Navarro, D.A. & Stortz, C.A. (2008) The system of xylogalactans from the red seaweed *Jania rubens* (Corallinales, Rhodophyta). *Carbohydrate Research*, 343, 2613–2622.
- Nishiyama, T., Sakayama, H., de Vries, J., Buschmann, H., Saint-Marcoux, D., Ullrich, K.K. et al. (2018) The *Chara* genome: secondary complexity and implications for plant terrestrialization. *Cell*, 174, 448–464.e24.
- Ogawa, K., Arai, M., Naganawa, H., Ikeda, Y. & Kondo, S. (2001) A new  $\beta$ -D-galactan having 3-O-methyl-D-galactose from *Chlorella vulgaris*. *Journal of Applied Glycoscience*, 48, 325–330.
- Ogawa, K., Yamaura, M. & Maruyama, I. (1994) Isolation and identification of 3-O-methyl-D-galactose as a constituent of neutral polysaccharide of *Chlorella vulgaris*. *Bioscience, Biotechnology, and Biochemistry*, 58, 942–944.
- Ogawa, K., Yamaura, M. & Maruyama, I. (1997) Isolation and identification of 2-O-methyl-L-rhamnose and 3-O-methyl-L-rhamnose as constituents of an acidic polysaccharide of *Chlorella vulgaris*. *Bioscience, Biotechnology, and Biochemistry*, 61, 539–540.
- O'Rourke, C., Gregson, T., Murray, L., Sadler, I.H. & Fry, S.C. (2015) Sugar composition of the pectic polysaccharides of charophytes, the closest algal relatives of land-plants: presence of 3-O-methyl-D-galactose residues. *Annals of Botany*, 116, 225–236.
- Palacio-López, K., Tinaz, B., Holzinger, A. & Domozych, D.S. (2019) Arabinogalactan proteins and the extracellular matrix of charophytes: a sticky business. *Frontiers in Plant Science*, 10, 447.
- Paulsen, B.S., Craik, D.J., Dunstan, D.E., Stone, B.A. & Bacic, A. (2014) The Yariv reagent: behaviour in different solvents and interaction with a gum arabic arabinogalactan-protein. *Carbohydrate Polymers*, 106, 460–468.
- Pedersen, H.L., Fangel, J.U., McCleary, B., Ruzanski, C., Rydahl, M.G., Ralet, M.-C. et al. (2012) Versatile high-resolution oligosaccharide microarrays for plant glycobiology and cell wall research. *Journal of Biological Chemistry*, 287, 39429–39438.
- Permann, C., Herburger, K., Felhofer, M., Gierlinger, N., Lewis, L.A. & Holzinger, A. (2021) Induction of conjugation and zygospore cell wall characteristics in the alpine *Spirogyra mirabilis* (Zygnematophyceae, Charophyta): advantage under climate change scenarios? *Plants*, 10, 1740.
- Permann, C., Herburger, K., Niedermeier, M., Felhofer, M., Gierlinger, N. & Holzinger, A. (2021) Cell wall characteristics during sexual reproduction of *Mougeotia* sp. (Zygnematophyceae) revealed by electron microscopy, glycan microarrays and RAMAN spectroscopy. *Protoplasma*, 258, 1261–1275.
- Pfeifer, L. & Classen, B. (2020) Validation of a rapid GC-MS procedure for quantitative distinction between 3-O-methyl- and 4-O-methyl-hexoses and its application to a complex carbohydrate sample. *Separations*, 7, 42.
- Pfeifer, L., Utermöhlen, J., Happ, K., Permann, C., Holzinger, A., von Schwarzenberg, K. et al. (2022) Search for evolutionary roots of land plant arabinogalactan-proteins in charophytes: presence of a rhamnogalactan-protein in *Spirogyra pratensis* (Zygnematophyceae). *The Plant Journal*, 109, 568–584.
- Popper, Z.A. & Fry, S.C. (2003) Primary cell wall composition of bryophytes and charophytes. *Annals of Botany*, 91, 1–12.
- Popper, Z.A., Sadler, I.H. & Fry, S.C. (2001) 3-O-methyl-D-galactose residues in lycophyte primary cell walls. *Phytochemistry*, 57, 711–719.
- Přerovská, T., Henke, S., Bleha, R., Spiwok, V., Gillarová, S., Yvin, J.-C. et al. (2021) Arabinogalactan-like glycoproteins from *Ulva lactuca* (Chlorophyta) show unique features compared to land plants AGPs. *Journal of Phycology*, 57, 619–635.
- Proseus, T.E. & Boyer, J.S. (2006) Calcium pectate chemistry controls growth rate of *Chara corallina*. *Journal of Experimental Botany*, 57, 3989–4002.
- Raimundo, S.C., Avci, U., Hopper, C., Pattathil, S., Hahn, M.G. & Popper, Z.A. (2016) Immunolocalization of cell wall carbohydrate epitopes in seaweeds: presence of land plant epitopes in *Fucus vesiculosus* L. (Phaeophyceae). *Planta*, 243, 337–354.
- Ralet, M.-C., Tranquet, O., Poulain, D., Moïse, A. & Guillon, F. (2010) Monoclonal antibodies to rhamnogalacturonan I backbone. *Planta*, 231, 1373–1383.
- Ruiz-May, E., Sørensen, I., Fei, Z., Zhang, S., Domozych, D.S. & Rose, J.K.C. (2018) The secretome and N-glycosylation profiles of the Charophycean green alga, *Penium margaritaceum*, resemble those of embryophytes. *Proteomes*, 6, 14.
- Ruprecht, C., Bartetzko, M.P., Senf, D., Dallabernadina, P., Boos, I., Andersen, M.C.F. et al. (2017) A synthetic glycan microarray enables



- epitope mapping of plant cell wall glycan-directed antibodies. *Plant Physiology*, 175, 1094–1104.
- Scheller, H.V. & Ulvskov, P. (2010) Hemicelluloses. *Annual Review of Plant Biology*, 61, 263–289.
- Seifert, G.J. & Roberts, K. (2007) The biology of arabinogalactan proteins. *Annual Review of Plant Biology*, 58, 137–161.
- Seifert, G.J., Strasser, R. & Van Damme, E.J.M. (2021) Editorial: plant glycobiology – a sweet world of glycans, glycoproteins, glycolipids, and carbohydrate-binding proteins. *Frontiers in Plant Science*, 12, 751923.
- Silva, J., Ferraz, R., Dupree, P., Showalter, A.M. & Coimbra, S. (2020) Three decades of advances in arabinogalactan-protein biosynthesis. *Frontiers in Plant Science*, 11, 610377.
- Smallwood, M., Yates, E.A., Willats, W.G.T., Martin, H. & Knox, J.P. (1996) Immunochemical comparison of membrane-associated and secreted arabinogalactan-proteins in rice and carrot. *Planta*, 198, 452–459.
- Sørensen, I., Pettolino, F.A., Bacic, A., Ralph, J., Lu, F., O'Neill, M.A. et al. (2011) The charophycean green algae provide insights into the early origins of plant cell walls. *The Plant Journal*, 68, 201–211.
- Staudacher, E. (2012) Methylation – an uncommon modification of glycans. *Biological Chemistry*, 393, 675–685.
- Stegemann, H. & Stalder, K. (1967) Determination of hydroxyproline. *Clinica Chimica Acta*, 18, 267–273.
- Steiner, P., Obwegeser, S., Wanner, G., Buchner, O., Lütz-Meindl, U. & Holzinger, A. (2020) Cell wall reinforcements accompany chilling and freezing stress in the streptophyte green alga *Klebsormidium crenulatum*. *Frontiers in Plant Science*, 11, 873.
- Suzuki, K. & Terasawa, M. (2020) Biological activities of rhamnan sulfate extracts from the green algae *Monostroma nitidum*. *Marine Drugs*, 18, 228.
- Taylor, R.L. & Conrad, H.E. (1972) Stoichiometric depolymerization of polyuronides and glycosaminoglycuronans to monosaccharides following reduction of their carbodiimide-activated carboxyl groups. *Biochemistry*, 11, 1383–1388.
- Thompson, E.W. & Preston, R.D. (1967) Proteins in the cell walls of some green algae. *Nature*, 213, 684–685.
- Timmins, A., Saint-André, M. & de Visser, S.P. (2017) Understanding how prolyl-4-hydroxylase structure steers a ferryl oxidant toward scission of a strong C–H bond. *Journal of the American Chemical Society*, 139, 9855–9866.
- Velasquez, S.M., Ricardi, M.M., Poulsen, C.P., Oikawa, A., Dilokpimol, A., Halim, A. et al. (2015) Complex regulation of prolyl-4-hydroxylases impacts root hair expansion. *Molecular Plant*, 8, 734–746.
- Verhertbruggen, Y., Marcus, S.E., Haeger, A., Ordaz-Ortiz, J.J. & Knox, J.P. (2009) An extended set of monoclonal antibodies to pectic homogalacturonan. *Carbohydrate Research*, 344, 1858–1862.
- Verhertbruggen, Y., Marcus, S.E., Haeger, A., Verhoef, R., Schols, H.A., McCleary, B.V. et al. (2009) Developmental complexity of arabinan polysaccharides and their processing in plant cell walls. *The Plant Journal*, 59, 413–425.
- Vlad, F., Tiainen, P., Owen, C., Spano, T., Daher, F.B., Oualid, F. et al. (2010) Characterization of two carnation petal prolyl 4 hydroxylases. *Physiologia Plantarum*, 140, 199–207.
- Voigt, J., Stolarczyk, A., Zych, M., Malec, P. & Burczyk, J. (2014) The cell-wall glycoproteins of the green alga *Scenedesmus obliquus*. The predominant cell wall polypeptide of *Scenedesmus obliquus* is related to the cell-wall glycoprotein gp3 of *Chlamydomonas reinhardtii*. *Plant Science*, 215–216, 39–47.
- Waterhouse, A., Bertoni, M., Bienert, S., Studer, G., Tauriello, G., Gumienny, R. et al. (2018) SWISS-MODEL: homology modelling of protein structures and complexes. *Nucleic Acids Research*, 46, W296–W303.
- Wickett, N.J., Mirarab, S., Nguyen, N., Warnow, T., Carpenter, E., Matasci, N. et al. (2014) Phylotranscriptomic analysis of the origin and early diversification of land plants. *Proceedings of the National Academy of Sciences of the United States of America*, 111, E4859–E4868.
- Woessner, J.P. & Goodenough, U.W. (1994) Volvocine cell walls and their constituent glycoproteins: an evolutionary perspective. *Protoplasma*, 181, 245–258.
- Yariv, J., Rapport, M.M. & Graf, L. (1962) The interaction of glycosides and saccharides with antibody to the corresponding phenylazo glycosides. *Biochemical Journal*, 85, 383–388.
- Yates, E.A., Valdor, J.F., Haslam, S.M., Morris, H.R., Dell, A., Mackie, W. et al. (1996) Characterization of carbohydrate structural features recognized by anti-arabinogalactan-protein monoclonal antibodies. *Glycobiology*, 6, 131–139.
- Yuasa, K., Toyooka, K., Fukuda, H. & Matsuoka, K. (2005) Membrane-anchored prolyl hydroxylase with an export signal from the endoplasmic reticulum. *The Plant Journal*, 41, 81–94.

## SUPPORTING INFORMATION

Additional supporting information can be found online in the Supporting Information section at the end of this article.

**How to cite this article:** Pfeifer, L., Mueller, K.-K., Utermöhlen, J., Erdt, F., Zehge, J.B.J., Schubert, H. et al. (2023) The cell walls of different *Chara* species are characterized by branched galactans rich in 3-O-methylgalactose and absence of AGPs. *Physiologia Plantarum*, 175(4), e13989. Available from: <https://doi.org/10.1111/ppl.13989>